International Journal of Pharmaceutics 669 (2025) 125038

Contents lists available at ScienceDirect

International Journal of Pharmaceutics

journal homepage: www.elsevier.com/locate/ijpharm

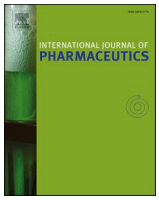

Core-shell aerogel design for enhanced oral insulin delivery

Gozde Ozesme Taylan [a], Carlos Illanes-Bordomás [b], Ozge Guven [c], Ece Erkan [c], Sevil Çıkrıkcı Erünsal [d,e], Mecit Halil Oztop [a,c], Carlos A. García-González [b,*]

[a] Department of Biotechnology, Graduate School of Natural and Applied Sciences, Middle East Technical University, Ankara, Turkey
[b] AerogelsLab, I+D Farma Group (GI-1645), Department of Pharmacology, Pharmacy and Pharmaceutical Technology, iMATUS and Health Research Institute of Santiago de Compostela (IDIS), Universidade de Santiago de Compostela, E-15782 Santiago de Compostela, Spain
[c] Department of Food Engineering, Middle East Technical University, Ankara, Turkey
[d] Department of Food Engineering, Konya Food and Agriculture University, Konya, Turkey
[e] Laboratory for Building Energy Materials and Components Swiss Federal Laboratories for Materials Science and Technology, EMPA, Dübendorf 8600, Switzerland

ARTICLE INFO

Keywords:
Core-shell aerogels
Drug delivery
Insulin
Pharmaceutical biotechnology
Supercritical CO_2

ABSTRACT

Current protein-based therapies often rely on intravenous and subcutaneous injections leading to patient discomfort due to the need for frequent administration. Oral administration route presents a more patient-friendly alternative, but overcoming the challenge of low drug bioavailability remains paramount. This limitation is primarily attributed to protein degradation in the harsh gastric environment, enzymatic breakdown, and poor intestinal permeability. With their unique properties, such as high porosity and surface area, and easy scalability, aerogels offer a promising platform for oral delivery of therapeutic proteins. This study focused on the development and characterization of both conventional and core–shell aerogels derived from natural polysaccharides for the oral delivery of insulin, utilizing *Humulin R*® U-100 as the insulin source for the first time. Aerogels were produced via supercritical carbon dioxide (sc-CO_2) drying of alginate gel beads. Scanning Electron Microscopy (SEM) images confirmed that the core–shell aerogels had higher uniformity in size and a more well-defined porous structure in comparison to conventional aerogels. Structural differences of two alginate sources were evaluated by Fourier Transform Infrared (FTIR) spectroscopy. A notable difference in encapsulation efficiencies was observed between conventional (12 %) and core–shell (53 %) aerogels, highlighting the superior carrier characteristics of the latter ones. *In vitro* insulin release profiles from the core–shell aerogels demonstrated their potential suitability for delivering regular/short-acting insulin therapeutics since only 30 % of insulin was released in Simulated Gastric Fluid (SGF) after 120 min, whereas 60 % of insulin was released in Simulated Intestinal Fluid (SIF) within the first hour followed by a sustained release stage.

1. Introduction

Insulin, a critical hormone responsible for regulating blood glucose levels, has long been administered via subcutaneous injections. However, the current standard of subcutaneous insulin injection (Alam et al., 2024) has been a source of distress and discomfort for many patients, highlighting the need for alternative delivery methods like oral and intranasal administration routes (Bashir et al., 2023). Namely, oral insulin delivery offers the potential to mimic the physiological insulin secretion patterns, improve patient compliance, and reduce the risk of hypoglycemia associated with injectable formulations (Arbit & Kidron, 2017; Khodaei et al., 2020).

Despite its potential, oral insulin delivery faces significant obstacles, primarily enzymatic degradation within the gastrointestinal tract and limited absorption across the intestinal epithelium (Cikrikci et al., 2018). To address these challenges, nanocarriers such as lipid-based and polymeric nanoparticles, can enhance the oral bioavailability of insulin (Iyer et al., 2022; Limenh, 2024; Zhang et al., 2021). Lipid nanocarriers, such as nanoemulsions and self-nanoemulsifying drug delivery systems (SNEDDS), can improve the permeability and stability of insulin, leading to increased intestinal absorption and reduced enzymatic degradation (Siram et al., 2019). Additionally, strategies like PEGylation and lipidization were employed to further enhance the oral delivery of insulin and GLP-1 receptor agonists (Poudwal et al., 2021). In another approach, polymeric nanoparticles can be designed to target specific transcytosis pathways in the intestinal epithelium, facilitating the

* Corresponding author.
E-mail address: carlos.garcia@usc.es (C.A. García-González).

https://doi.org/10.1016/j.ijpharm.2024.125038
Received 1 October 2024; Received in revised form 2 December 2024; Accepted 3 December 2024
Available online 5 December 2024

transport of insulin and other therapeutic agents across the gastrointestinal barrier and into the systemic circulation (Zhang et al., 2021).

Aerogel carriers are herein regarded as an alternative for the oral delivery of insulin. Aerogels are highly porous, lightweight materials with a high surface area, making them suitable for drug encapsulation and controlled release (García-González et al., 2011; Illanes-Bordomás et al., 2023). Compared to traditional silica-based aerogels, polysaccharide-based aerogels can offer improved mechanical properties and enhanced biological functionality. The typical process for producing aerogels from polysaccharides includes producing a hydrogel, a solvent exchange (typically to ethanol), and the subsequent drying of the gel using supercritical carbon dioxide (sc-CO_2). Sc-CO_2 drying is a crucial step, as it allows for the removal of the liquid phase from the gel structure without causing significant shrinkage or density increase, resulting in the preservation of the high porosity and a low density in the final aerogel (Ajdary et al., 2021). In this context, polysaccharide-based aerogels have emerged as a promising platform for the oral delivery of drugs, including insulin (Abdul Khalil et al., 2023; García-González et al., 2021, 2015). In the case of aerogels for insulin oral delivery, chitosan and alginate aerogels possess mucoadhesive properties (Amin and Boateng, 2022; Ways et al., 2018), which can enhance the residence time of the insulin-loaded aerogels within the gastrointestinal tract, thereby improving drug absorption.

Conventional drug-loaded aerogel production includes the loading of the drug into the aerogel structure uniformly (García-González et al., 2021). The production of conventional aerogels involves a multi-step process that begins with gel formation, usually achieved dropping the solution containing the gel precursor and the drug into the crosslinking bath via automatic syringe pump and the resulting gel undergoes sc-CO_2 drying. An innovative approach is the development of core–shell aerogels with a biopolymer-based core and a functionalized shell as drug delivery systems offering several benefits. The co-axial prilling technique is the primary method for fabricating core–shell aerogel particles. Using co-axial prilling and sc-CO_2 drying, De Cicco et al. produced core–shell aerogels loaded with doxycycline utilizing alginate and amidated pectin for wound healing (De Cicco et al., 2016). The core–-shell structure enabled controlled or delayed release profiles, achieving favorable encapsulation efficiencies, high surface area, and enhanced pore structure provided by sc-CO_2 drying. These characteristics highlight the suitability of the core–shell structure for drug delivery applications.

This work evaluates the potential of polysaccharide-based aerogels as novel drug carriers for oral delivery of insulin. This is the first systematic study to explore the feasibility of using polysaccharide-based aerogels for the oral delivery of regular/short-acting insulin. Core-shell aerogel beads, which were used as oral drug delivery agent for the first time, loaded with insulin in the core were produced, and their performance was compared to that of insulin uniformly loaded in conventional alginate aerogel particles. The physicochemical characterization (SEM microscopy, nitrogen adsorption–desorption analysis, FTIR spectroscopy) of polysaccharide-based core–shell and conventional aerogels from different alginate sources, their ability to encapsulate (drug loading efficiency by HPLC), and the evaluation of *in vitro* insulin release profiles of core–shell aerogels (in SGF, SIF and SCF media) were carried out.

2. Materials and methods

2.1. Materials

Sodium alginate denoted as ALG-1 (alginic acid sodium salt from brown algae, medium viscosity, M/G ratio: 1.56, degree of polymerization: 400–600, MW: *ca.* 250–350 kDa) was purchased from Sigma (Irvine, UK). Sodium alginate denoted as ALG-2 (sodium alginate, M/G ratio: 1.56, MW: *ca.* 12–40 kDa) was purchased from Merck (Darmstadt, Germany). Calcium chloride anhydrous (MW: 110.99 g/mol) was purchased from Scharlau (Barcelona, Spain). Chitosan was purchased from Merck (deacetylation degree 75–85 %, MW: *ca.* 190–300 kDa, Darmstadt, Germany). *Humulin R*® U-100 (Eli Lilly & Company, Indianapolis, IN, USA) was purchased from a local pharmacy in the form of 10-mL vials containing human insulin (see composition in Table 1) and used for all drug-loaded particles. Carbon dioxide (CO_2 > 99.8 % purity) was supplied by Nippon Gases (Madrid, Spain) and Linde (Gebze, Türkiye). Absolute ethanol from Merck (Darmstadt, Germany) and ISOLAB Laborgeräte GmbH (Eschau, Germany), acetic acid glacial from Scharlau (Barcelona, Spain) and ISOLAB Laborgeräte GmbH (Eschau, Germany), potassium dihydrogen phosphate and sodium dihydrogen phosphate from Merck (Darmstadt, Germany) were used throughout the experiments.

Table 1
Active pharmaceutical ingredient and excipients of Humulin R® in 10-mL vials (U.S. Food and Drug Administration, 2011).

Human Insulin (rDNA origin)	100 units/mL (3.5 mg/mL)
Meta-cresol	2.5 mg/mL
Glycerin	16 mg/mL
Endogenous Zinc	0.0015 mg/100 units
Water for injection	Total volume of vial

2.2. Preparation of blank and drug-loaded conventional gel beads

For blank conventional gel beads, two different alginate aqueous solutions with concentrations between 1.5–2.5 % w/v were prepared and tested for bead formation. 1.5 % w/v for ALG-1 and 2.0 % w/v for ALG-2 were selected as they provided better control on the bead size and shape using the automatic syringe. Then, two different aqueous crosslinking baths (CB-1, chitosan (0.4 %, w/v) and 0.5 M $CaCl_2$ dissolved in 1 % v/v acetic acid; CB-2, 0.5 M $CaCl_2$ solution in distilled water) were prepared in deionized water. CB-1 solution was prepared by using UltraTurrax T-18 (IKA, Staufen im Breisgau, Germany) for 2 min and stirred for at least 2 h at room temperature. Then, $CaCl_2$ was added and stirred at room temperature until it dissolved. For the CB-2 solution, $CaCl_2$ was added to distilled water and stirred at room temperature until $CaCl_2$ dissolved (*ca.* 30 min). 20 mL of the alginate solutions were dropped into 100 mL of CB-1 or CB-2 gelation baths using an automatic syringe pump (Inovenso, Boston, MA, USA) at a flow rate of 3 mL/min. Hydrogels were immediately formed after contact with the alginate solution droplets in the gelation baths. After 10 min in crosslinking baths for aging, hydrogel particles were removed, washed gently with water, and put into ethanolic baths of 10 mL. Hydrogels were sequentially placed into 50 % v/v and 80 % v/v ethanol baths for 10 min. Then, gels were put into absolute ethanol for 48 h to obtain the alcogel beads.

To produce drug-loaded hydrogel beads, ALG-1 was dissolved in 10 mL *Humulin R*® (100 units/mL) so that the ALG-1 and insulin concentrations were 1.5 % w/v and 3.5 mg/mL, respectively. The solution containing the insulin was dropped using an automatic syringe at 3 mL/min into the CB-1 and CB-2 baths. A similar process for ALG-2 with concentration of 2.0 % w/v and CB-1 bath for crosslinking. The following steps were the same as those for the production of blank conventional alcogel beads.

2.3. Preparation of blank and drug-loaded core-shell gel beads

A co-axial prilling nozzle system (Encapsulator Unit Var J1, Nisco Engineering AG, Zurich, Switzerland) was used to prepare the core–shell gel beads as it is seen in Fig. 1. ALG-1 solution at 1.5 % w/v was prepared as core solution, and ALG-1 was prepared at 2.0 % w/v as shell solution. CB-1 was used as the crosslinking bath. Alginate core solution was pumped at a rate of 0.058 g/min, and a pressure of 0.9 bar through the inner orifice (0.35 mm) of the co-axial nozzle, and the alginate shell solution was pumped at a rate of 0.66 g/min and a pressure of 1.2 bar by the outer orifice (0.80 mm) of the same nozzle. The compressed air flow

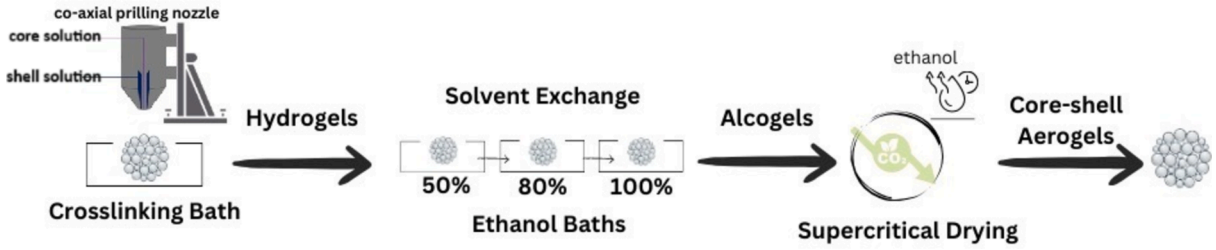

Fig. 1. Sketch showing the core–shell aerogel production process.

rate was set to 1.5 L/min. The obtained droplets were crosslinked immediately after contact with the gelation bath and aged for 10 min. Afterwards, the obtained hydrogel beads were taken from the bath, and a similar solvent exchange procedure was followed as in Section 2.2.

To produce drug-loaded core–shell hydrogel beads, 0.6 g of ALG-1 was dissolved in 40 mL *Humulin R*® (100 units/mL, Table 1) so that the ALG-1 and insulin concentrations were 1.5 % w/v and 3.5 mg/mL, respectively. The resulting solution was kept under magnetic stirring (80 rpm, 2 h) until further use. After the drug was entirely dissolved in the alginate solution, the same procedure was followed to obtain the insulin-loaded core–shell gel beads as for the blank core–shell beads abovementioned.

2.4. Supercritical CO_2 drying for aerogel production

For the drying of conventional alcogel beads via sc-CO_2, the alcogel beads were dried using a supercritical dryer with a 500 mL extraction column (Superex F-500, Konya, Türkiye). The drying process involved a sc-CO_2 flow rate of 3.3 g/min for 1.5 h, conducted at a temperature of 35 °C and a pressure of 200 bar.

For the drying of core–shell alcogel particles with sc-CO_2, the different batches of alcogels were introduced into paper cartridges and subsequently placed into a 100 mL high-pressure autoclave (Waters-Thar Process, Pittsburg, PA, USA). Then, the autoclave was pressurized until 120 bar at 37°C, and the gel samples were supercritical dried for 3.5 h at a flow rate of 5–7 g/min (Carracedo-Pérez et al., 2024). Then, the autoclave was depressurized.

In both drying cases, the aerogels were collected from the autoclaves preserving the original porous structure and removing the ethanol completely. The notation of the aerogels used in this study and their corresponding short names are given in Table 2.

2.5. Characterization and performance evaluation

2.5.1. Fourier-Transform Infrared spectroscopy (FTIR)

FTIR analysis was performed for raw alginates, chitosan, CS-B and CS-D by using Shimadzu IRTracerTM-100 Fourier Transform Infrared Spectrometer (Shimadzu Corporation, Kyoto, Japan) in the 4000–400 cm^{-1} wavenumber range at a resolution of 16 cm^{-1} and 32 scans.

2.5.2. Rheological measurements of alginate solutions

Viscosity measurements were conducted at 25 °C using a Brookfield Ametek RST-CC Rheometer (Middleborough, MA, USA) equipped with a bob-and-cup geometry (bob radius: 12.5 mm, cup radius: 13.56 mm, angle: 120°). The experiments covered a shear rate range of 0.10 to 1200 s^{-1}. Shear stress (σ in Pa) and apparent viscosity (Pa·s) results were measured. Data were fitted to the Power Law model (Eq. (1)):

$$\sigma = K \times \gamma^n \tag{1}$$

where γ is the shear rate (1/s), K is the flow consistency index ($Pa{\cdot}s^n$), and n is the flow behavior index (Balmforth and Craster, 2001).

Table 2
Aerogel formulation notation.

Aerogel formulation	Codes
Core-shell blank aerogels	CS-B
Core-shell drug-loaded aerogels	CS-D
Blank conventional aerogels with ALG-1 in CB-1	CA-11B
Blank conventional aerogels with ALG-1 in CB-2	CA-12B
Blank conventional aerogels with ALG-2 in CB-1	CA-21B
Drug-loaded conventional aerogels with ALG-1 in CB-1	CA-11D
Drug-loaded conventional aerogels with ALG-1 in CB-2	CA-12D
Drug-loaded conventional aerogels with ALG-2 in CB-1	CA-21D

2.5.3. Scanning Electron microscopy (SEM)

SEM imaging was performed on the aerogel formulations using a QUANTA 400F Field Emission SEM (Hillsboro, OR, USA) at an accelerating voltage of 5 kV and a magnification of 40,000x. Prior to imaging, aerogels were coated with gold and mounted on conductive tape.

2.5.4. Nitrogen adsorption-desorption analysis

Prior to analysis, the aerogel samples underwent a degassing procedure under vacuum (<1 mPa) at 50 °C for 24 h, and then nitrogen adsorption–desorption analysis was performed at 77 K (ASAP 2000, Micromeritics Inc.; Norcross, GA, USA). Brunauer-Emmett-Teller (BET) model was used for specific surface area determination, and the Barrett-Joyner-Halenda (BJH) model was used for specific pore volume and mean pore size distribution determinations.

2.5.5. Drug loading capacity (DLC) and encapsulation efficiency (EE)

Insulin-loaded aerogels (*ca.* 18 mg) were dissolved in 10 mL of PBS solution (pH 7.4), and the insulin content was analyzed in reverse-phase high-performance liquid chromatography RP-HPLC (Shimadzu Sci. Ins., Kyoto, Japan) consisting of ReproSil-Pur 120 C18-AQ column to determine the amount of insulin. A flow rate of 1.0 mL/min was maintained for isocratic elution using a mobile phase composed of acetonitrile and 10 mM phosphate buffer (pH 3.0) in a 50:50 v/v ratio. A 20 µL sample volume was injected, and UV detection was performed at the wavelength of 214 nm. 10.0 mM phosphate buffer was prepared by dissolving 1.56 g of sodium dihydrogen phosphate (NaH_2PO_4) in approximately 800 mL of water, adjusting the pH to 3.0 with o-phosphoric acid, and bringing the final volume to 1000 mL with water (Nenni, 2021). The insulin concentration was calculated based on a calibration curve made with different concentrations of the drug (2.5 % to 15 %) in PBS pH 7.4 medium with R^2=0.993. Drug loading capacity (DLC) and encapsulation efficiency (EE) (Zatorska et al., 2020) were used for the loading performance evaluation using Eqs. (2) and (3), respectively.

$$DLC\% = \left(\frac{Mass\ of\ drug\ in\ aerogel}{Total\ mass\ of\ aerogel}\right) \times 100 \tag{2}$$

$$EE\% = \left(\frac{Experimental\ drug\ mass\ in\ aerogel}{Theoretica\ ldrug\ mass\ added}\right) \times 100 \tag{3}$$

2.6. Drug release experiments

Since initial findings indicated that enzymes in the release media led to the swift breakdown of insulin, simulated gastric fluid (SGF),

simulated intestinal fluid (SIF), and simulated colonic fluid (SCF) media were prepared without enzymes (Cikrikci et al., 2018). To prepare the SGF medium, 3 g NaCl was dissolved in 1450 mL water and adjusted pH to 1.2 with diluted HCl. For the SIF medium, 6.8 g KH_2PO_4 dissolved in 250 mL water, then 77 mL 0.2 N NaOH was added, and the final volume reached 1 L with a pH of 6.8. For the colonic environment, the solution pH was adjusted to 7.4 using the same procedure used in SIF.

Drug-loaded aerogels were put into 30 mL of SGF medium at 37 °C and 100 rpm, and aliquots of 1 mL were taken using a pipette at different time points (15 min, 30 min, 1 h and 2 h). To assess insulin release in SIF medium, drug-loaded aerogels were put into 30 mL of SIF medium at 37 °C and 100 rpm, and aliquots were taken at different time points (30 min, 1, 2, 3, 4, 5 and 6 h). To assess insulin release in SCF medium, drug-loaded aerogels were put into 30 mL of SCF medium at 37 °C and 100 rpm, and aliquots were taken after 30 min, 1, 2, 3, 4, 5 and 6 h. After taking aliquots, the same amount of fresh release medium was added in all cases. Release tests were carried out in triplicate for the three release media used and *ca.* 0.1 g of drug-loaded aerogels were used for each test.

All aliquots from the release tests were analyzed by RP-HPLC, with the method described in Section 2.5.5. The insulin concentration in the different release media was calculated with calibration curves of insulin in all three release media, previously prepared with known concentrations (2.5 % to 15 % w/v) of insulin drug standard solutions and m-cresol ($R^2 = 0.995$ in SGF, $R^2 = 0.999$ in SIF and $R^2 = 0.998$ in SCF). All HPLC measurements were performed in at least three replicates.

2.7. Statistical analysis

Data were analyzed using one-way ANOVA tests in Minitab v19.1 (Coventry, UK) software. Significant differences between groups were determined using Tukey's post-hoc comparison test with a significance level of $p < 0.05$. The assumptions of ANOVA tests were verified before conducting the analysis. Different letters in the figures and tables represent statistically significant differences between the experimental sample groups.

3. Results and discussion

3.1. Chemical and rheological characterization of alginate solutions

Fig. 2 shows the FTIR spectra of ALG-1 and ALG-2. Both alginates showed similar main absorbance bands. The band at around 1000–1100 cm^{-1} reflects the C-O-C stretching vibrations typical of glycosidic bonds, the chemical links within polysaccharides (Valentin et al., 2007). Furthermore, both showed a peak around 1600 cm^{-1} that represents the symmetric stretching vibration of carboxylate O–C–O and around 1400 cm^{-1} related to the symmetric stretching vibration of the carboxylate group (Rashedy et al., 2021). Both alginates had broad peaks around 3200–3500 cm^{-1}. This represents hydrogen bonding and hydroxyl groups available (Nandiyanto et al., 2023) for interactions which could affect the gel formation and drug encapsulation. To better compare the spectra based on intensities, they were adjusted based on the C-O stretching band (1020–1080 cm^{-1}). This band represents the unchanging backbone of alginate and serves as a stable reference point (Pereira et al., 2011), minimizing intensity variations between samples. Subsequently, spectra showed that the chemical structures of ALG-1 and ALG-2 were very similar. Therefore, both alginates were considered alternative polysaccharides in aerogel production.

The rheological behavior of the two different alginate solutions at two different concentrations has a considerable effect on hydrogel production and further aerogel properties. The flow behavior of alginate solutions results (Fig. 3) showed that the consistency index, K values were 5.45 and 17.70 $Pa{\cdot}s^n$ for ALG-1 and 0.08 and 0.11 $Pa{\cdot}s^n$ for ALG-2,

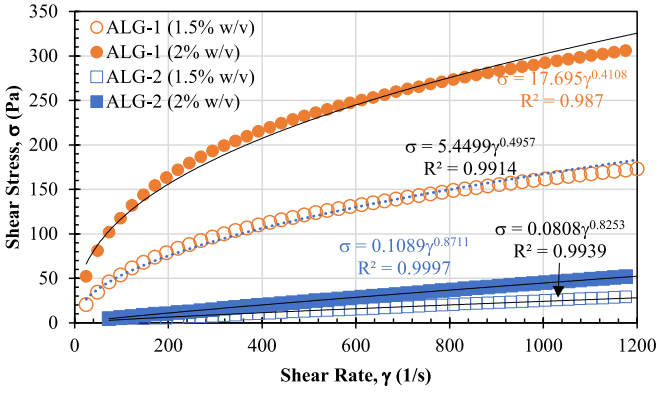

Fig. 3. Rheological analysis of ALG-1 (1.5 % w/v and 2 % w/v) and ALG-2 (1.5 % w/v and 2 % w/v) aqueous solutions.

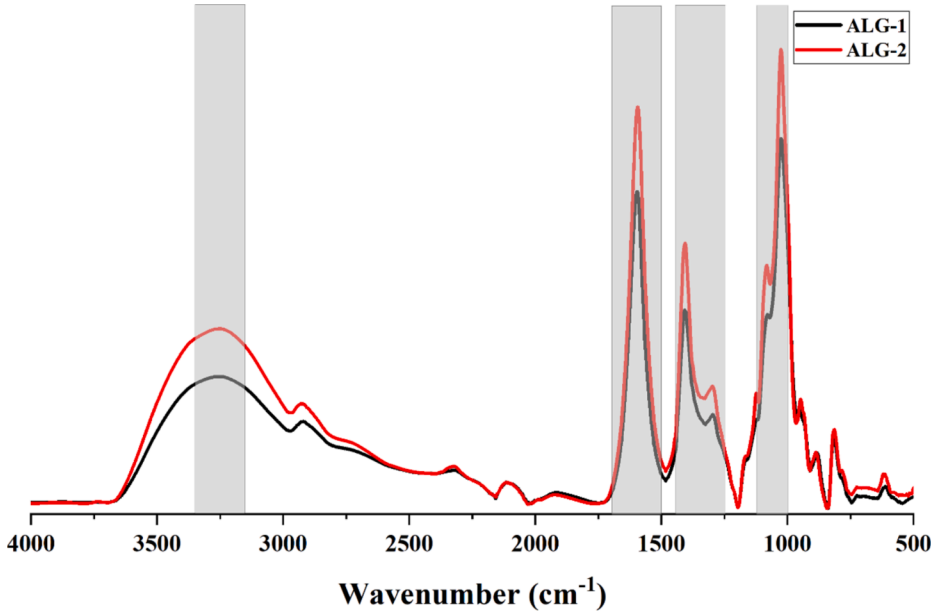

Fig. 2. FTIR spectra of ALG-1 and ALG-2. Highlighted grey areas mark main absorbance bands.

at concentrations of 2 % w/v and 1.5 % w/v, respectively. In addition, the flow behavior index (n) values were 0.50 and 0.41 for ALG-1 and 0.83 and 0.87 for ALG-2 at the same concentrations. Thus, ALG-1 solution showed a significant increase in shear stress with increasing shear rate, while ALG-2 solution showed a much more gradual increase in shear stress with increasing shear rate. ALG-1 solution indicated a strong correlation and suggested a non-Newtonian behavior, specifically shear-thinning ($n < 1$), where the viscosity decreases with increasing shear rate. On the other hand, ALG-2 solution indicated an almost linear behavior (n being close to 1) but still shear-thinning to a lesser extent than ALG-1 solution. The significant shear-thinning behavior suggests that ALG-1 solution would provide better control on the bead size and shape than ALG-2 solution at both concentrations.

The solutions of ALG-1 showed a significantly higher K value compared to ALG-2. Higher K value in alginate solutions leads to a denser and more stable gel network, which might improve the

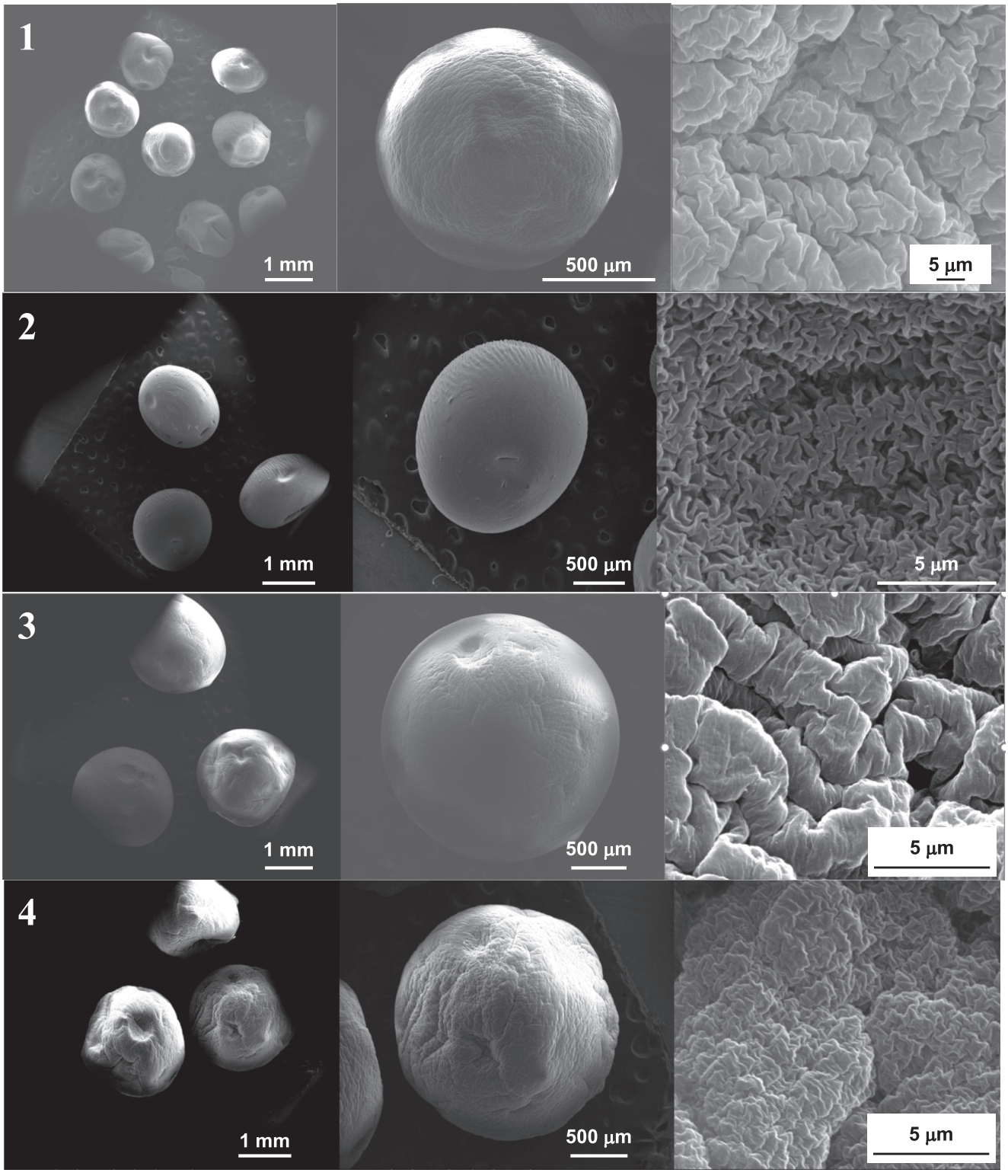

Fig. 4. SEM images of (1) CS-B, (2) CA-21B, (3) CA-12B, and (4) CA-11B aerogels. Scale bars: 1 mm (left), 500 µm (middle), 5 µm (right).

encapsulation efficiency but can also make the drug-loading process more challenging due to increased resistance to mixing.

The rheological properties provided a deeper understanding of the different performances of ALG-1 and ALG-2 in drug encapsulation processes. Shear thinning fluids exhibit a decrease in viscosity with increasing shear rate, a property that can be particularly beneficial in the co-axial prilling process (Levato et al., 2020). The shear-thinning nature of the polymer solution benefits the extrusion and co-extrusion process. As shear forces increase during prilling, the viscosity of the fluid decreases, allowing for smoother flow. Therefore, ALG-1 and ALG-2 solutions were both used to produce conventional aerogels, whereas ALG-1 was used for the core part of the core–shell aerogel production with the concentration of 1.5 % w/v since the tips of the nozzles were clogged with higher concentrations due to their higher viscosities.

3.2. Morphological characterization of aerogels

As preliminary tests, 1.5 % w/v and 2 % w/v concentrations of alginate solutions (both ALG-1 and ALG-2) were dropped into the crosslinking bath (CB-1) with an automatic syringe pump for hydrogel production. The alginate concentrations of 1.5 % w/v for ALG-1 and 2.0 % w/v for ALG-2 were selected for ulterior conventional gel formation tests according to the criterion of giving a more spherical hydrogel shape. Following the successful formation of spherical hydrogel beads using these concentrations, both core–shell and conventional aerogels were produced via sc-CO_2 drying.

Fig. 4 shows the SEM images of CS-B, CA-21B, CA-12B and CA-11B providing a visual representation of the aerogel characteristics: morphology (left), representative spherical particles (middle), and porous structure and surface roughness (right). CS-B aerogels are the best choice due to its high uniformity in size, more spherical shape, and better porous surface, all required for consistent and efficient drug loading. CA-21B and CA-12B aerogels also showed good uniformity and a relatively smooth and porous surface, making them a strong drug delivery candidate among conventional aerogels.

All the isotherms of the aerogels (Fig. 5) obtained by nitrogen adsorption–desorption analysis show a hysteresis loop providing evidence that these aerogels possess a predominantly mesoporous structure (Awoke et al., 2020). Mesopores can significantly impact drug loading capacity and efficiency. Their high specific surface area facilitates increased drug adsorption or encapsulation, while the tunable pore sizes accommodate a wide range of drug sizes, enhancing loading capacity and enabling controlled release via diffusion-controlled mechanisms (Tkalec et al., 2016).

The pore size distribution plot (volume vs. pore diameter) was calculated from the desorption data by the BJH model (Fig. 6). CS-B exhibits a predominantly mesoporous structure with uniform pore sizes, indicated by a sharp peak at small diameters. This suggests a high surface area, beneficial for applications like small molecule adsorption like insulin. Conversely, CA-11B and CA-12B displayed broader peaks,

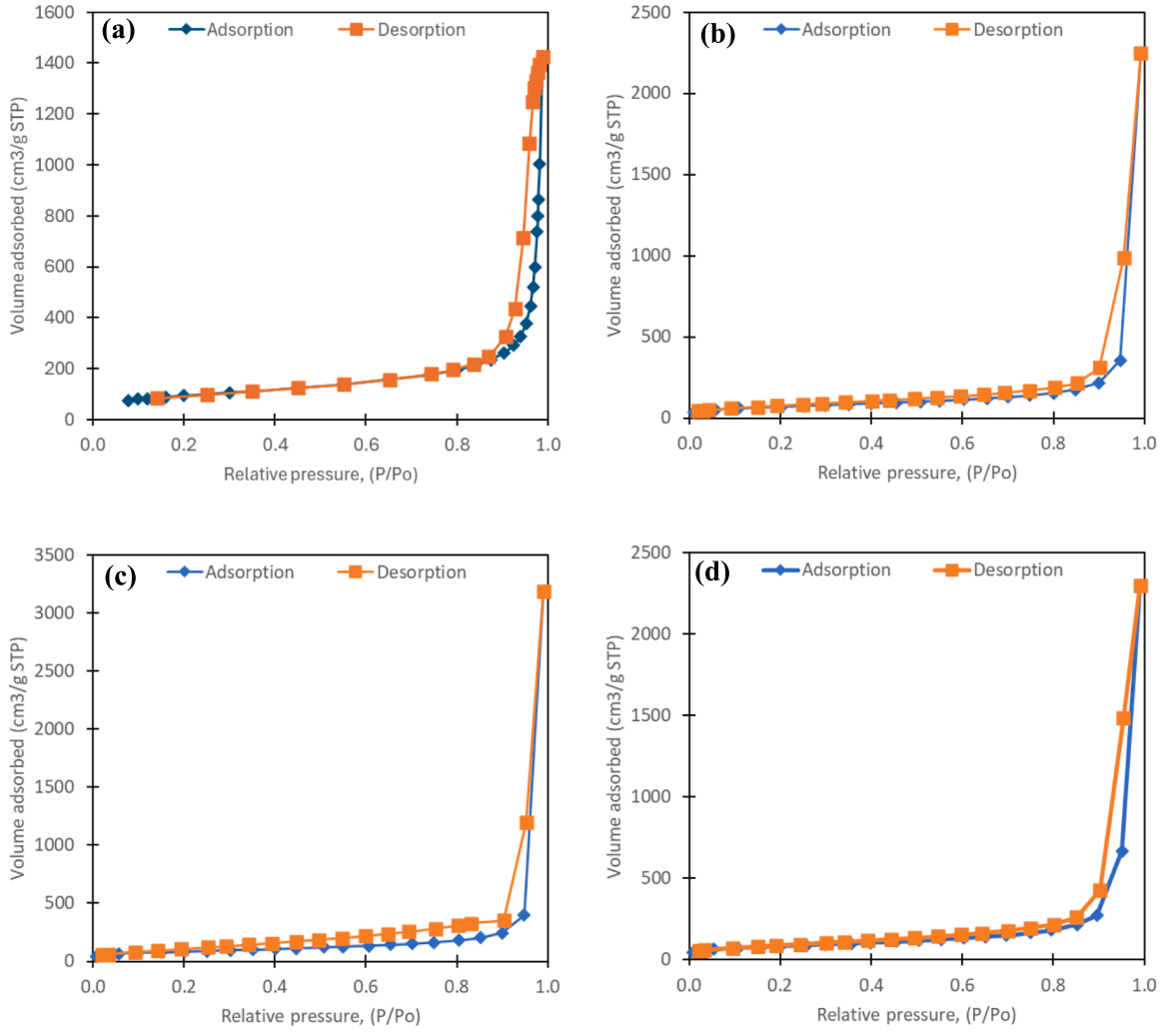

Fig. 5. Nitrogen adsorption–desorption isotherms of (a) CS-B, (b) CA-11B, (c) CA-12B and (d) CA-21B aerogel formulations.

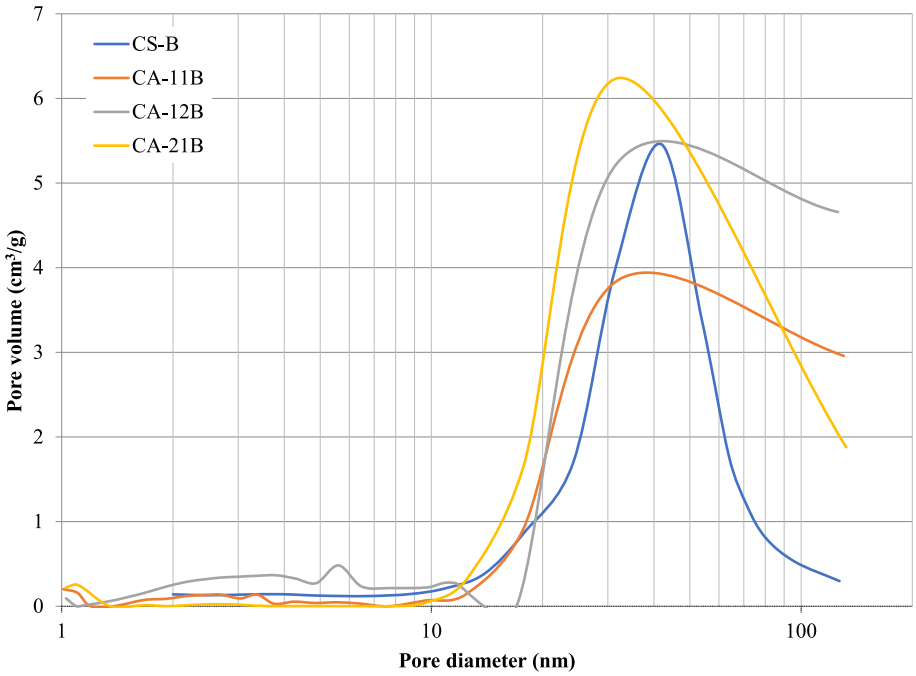

Fig. 6. Pore size distribution of blank alginate aerogels measured by the nitrogen desorption method.

with CA-12B shifted towards higher diameters, suggesting larger mesopores and some macropores. Table 3 provides the specific surface area, mean pore diameter, and specific pore volume for the different blank aerogels. An increased surface area for an aerogel of similar composition usually correlates to a higher capacity for drug adsorption, as the higher surface provides more potential binding sites for the drug molecules (García-González et al., 2021). The core–shell aerogel (CS-B) exhibited a higher surface area than conventional aerogels and is anticipated to demonstrate a higher capacity for drug loading. The pore diameter can affect the rate at which the drug is released. Larger pores, like CA-11B, may facilitate faster drug release rates, which might be beneficial for drugs requiring rapid-acting insulin. Smaller pores can provide a more controlled and sustained release, which would be advantageous for maintaining therapeutic levels over time such as for regular/short-acting insulin analogs, like *Humulin R®*.

3.3. Evaluation of the performance of the insulin-loaded aerogels

The experimental insulin amount in the aerogels was determined by HPLC analysis, and the DLC and EE values of the aerogels were calculated (Table 4) to evaluate the loading process performance. The changes in alginate source (ALG-1 or ALG-2) and crosslinking bath (CB-1 or CB-2) on conventional aerogels did not show significant differences regarding their effect on DLC and EE values.

Significant differences in DLC and EE were obtained between core–shell drug-loaded aerogels (CS-D) and conventional drug-loaded aerogels (CA-11D, CA-12D and CA-21D). CS-D aerogel exhibited the highest DLC and EE values (Table 4). The core–shell structure likely provides a more controlled environment for drug encapsulation, reducing drug loss after the gelation step, namely during the aging, solvent exchange, and drying processing steps to obtain the aerogels. The results demonstrated the superior ability of core–shell aerogels to incorporate and retain the drug compared to conventional aerogels.

Core-shell aerogel type was chosen for *Humulin R®* release investigation as a result of its 4-fold higher insulin encapsulation efficiency, the highest surface area obtained from N_2 adsorption–desorption analysis among the formulations tested and its mesoporous structure. Although the presence of chitosan in crosslinking baths did not make a significant contribution to the encapsulation efficiency and aerogel morphology, the production of CS-D was continued with CB-1 as the presence of chitosan can provide a pH-responsive behavior (Shu and Zhu, 2002) that would be beneficial for controlling drug release.

FTIR analysis was employed to confirm the successful incorporation of insulin into the core–shell aerogels by examining the spectral features of CS-D and CS-B, as it is shown in Fig. 7. CS-B spectra exhibited characteristic peaks of ALG-1 and chitosan. The subtle peak observed around 1690 cm^{-1} in the CS-B spectrum could be attributed to the amide I band of chitosan (Namli et al., 2023) from the crosslinking bath, a characteristic not present in alginate. While CS-D retained alginate functional groups, significant changes were observed in the amide I and II regions. Amide I (~1650 cm^{-1}) associated with C = O stretching and amide II

Table 3
Results of nitrogen adsorption–desorption analysis of blank (unloaded) alginate aerogels.

Aerogel Type	BET-Specific Surface Area (m^2/g)	BJH-desorption Average Pore Diameter (nm)	BJH-desorption Specific Pore Volume (cm^3/g)
CS-B	337.7 ± 17.0	25.44 ± 1.27	2.21 ± 0.11
CA-11B	245.5 ± 12.0	36.55 ± 1.83	3.53 ± 0.18
CA-12B	293.2 ± 12.0	33.27 ± 1.66	5.05 ± 0.25
CA-21B	287.8 ± 14.0	33.65 ± 1.68	3.62 ± 0.18

Table 4
EE and DLC values for insulin of the drug-loaded aerogels.

Aerogel type		DLC (%)*	EE (%)*
Core-shell drug-loaded aerogels	CS-D	5.9 ± 0.44[a]	53.7 ± 4.00[a]
Drug-loaded conventional aerogels with ALG-1 in CB-1	CA-11D	2.3 ± 0.15[b]	12.9 ± 0.86[b]
Drug-loaded conventional aerogels with ALG-1 in CB-2	CA-12D	2.5 ± 0.27[b]	13.3 ± 1.54[b]
Drug-loaded conventional aerogels with ALG-2 in CB-1	CA-21D	3.4 ± 0.20[b]	12.6 ± 0.74[b]

* Different letters indicate significant differences among the aerogel formulations ($p < 0.05$).

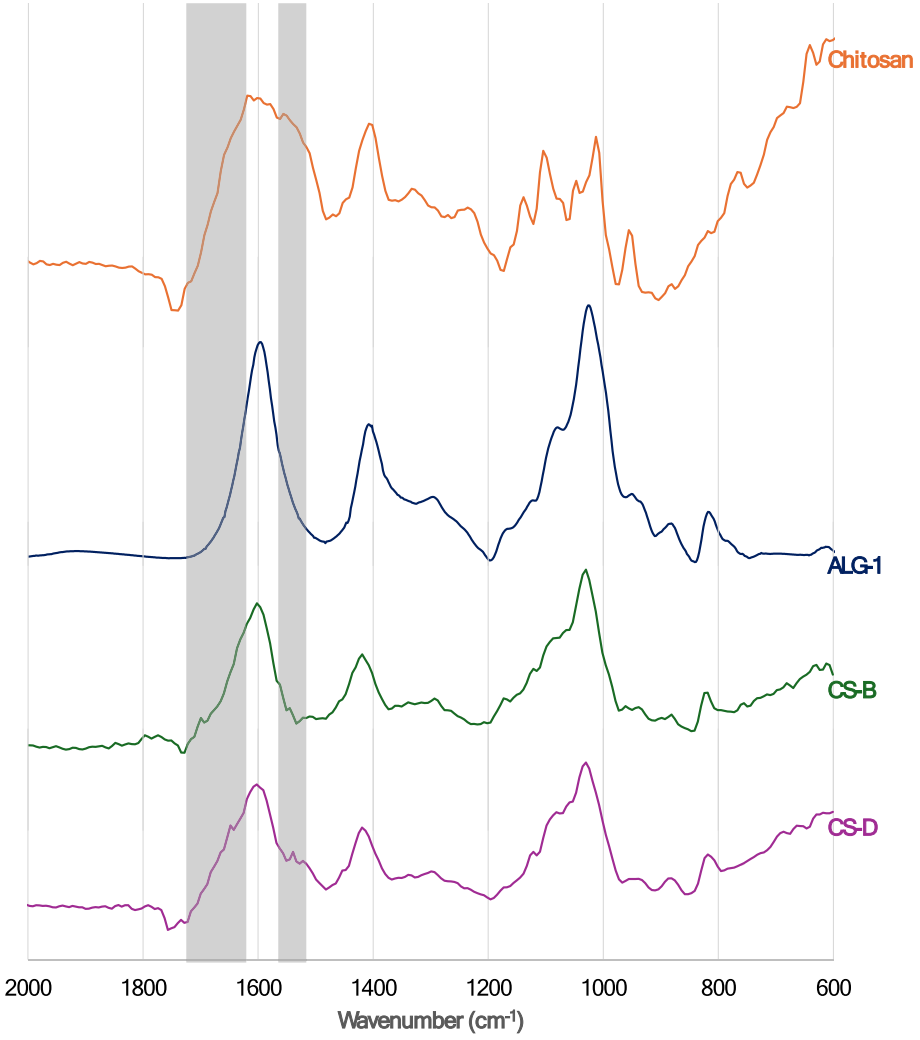

Fig. 7. FTIR spectra of chitosan, ALG-1, blank core–shell aerogels (CS-B) and drug-loaded core–shell aerogels (CS-D).

(~1550 cm^{-1}) related to N–H bending and C-N stretching in proteins (Sarmento et al., 2006). The notable change especially in the amide II regions confirmed the presence of insulin and indicated interactions between insulin and the aerogel matrix, likely through electrostatic interactions or hydrogen bonding involving C = O and N–H groups (Jamshidnejad-Tosaramandani et al., 2023). These findings confirm insulin loading without compromising the structural integrity of the aerogel.

Fig. 8 shows the cumulative insulin release profile from core-shell aerogels in three different *in vitro* simulated (gastric, intestinal and colonic) environments: SGF pH 1.2, SIF pH 6.8 and SCF pH 7.4.

In this study, the insulin release in SGF medium remained relatively low and constant, reaching a plateau at about 35 % after 120 min. In environments mimicking the low pH of the stomach, alginate alone can effectively limit drug release (Ching et al., 2008). This is because the carboxyl groups within the alginate structure become protonated in acidic conditions, causing the alginate to shrink and become more compact. The literature highlights research exploring how modifying alginate or incorporating another polymer influences drug release from nanoparticulate and microparticulate forms (Cao et al., 2019; El-Sherbiny, 2010; Kulkarni et al., 2012; Li et al., 2022). Specifically, a total amount of drug released in SGF medium in the 14–30 % range was reported. Therefore, the low release in SGF medium herein observed indicates that the core–shell aerogels are stable in acidic conditions. This stability is crucial for protecting the loaded insulin in the particles, so CS-D can effectively shield the insulin and prevent premature release, which is essential for oral drug delivery systems aiming to deliver active pharmaceuticals beyond the stomach.

In the SIF medium, the release profile showed a burst insulin release, reaching approximately 60 % within the first hour. Then, the drug release continued at a lower pace from 60 to 360 min, suggesting that the remaining insulin was released more slowly, likely from the core of the aerogel. Under exposure to environments with a neutral or slightly basic pH, pure alginate matrices demonstrated a notable increase in drug release (Uyen et al., 2020). This enhanced release was attributed to the ionization of carboxyl groups within the alginate structure. This ionization led to increased water uptake and swelling, creating a more porous matrix that facilitated drug diffusion. However, studies investigating drug release from alginate-based particles in SIF medium showed a wide range of results in the literature (Bensouiki et al., 2020; Cao et al., 2019; Imanishi et al., 2024; Thomas et al., 2021). Typically, chemical modifications made to the alginate and the use of different copolymers led to a drug release ranging from 40 % to 80 % within the initial two hours, i.e., within the range of this work. The combination of an initial burst insulin release followed by a sustained release stage optimizes therapeutic outcomes and enhances patient compliance, making it a suitable delivery system for *Humulin R*®. The initial rapid release phase observed in the core–shell aerogels can be particularly beneficial for rapidly or short-acting insulins like *Humulin R*®, the insulin source in this study, designed to start lowering blood glucose levels within 30 min of administration. The peak hour of release in the SIF medium was approximately the third hour, which is consistent with the expectation

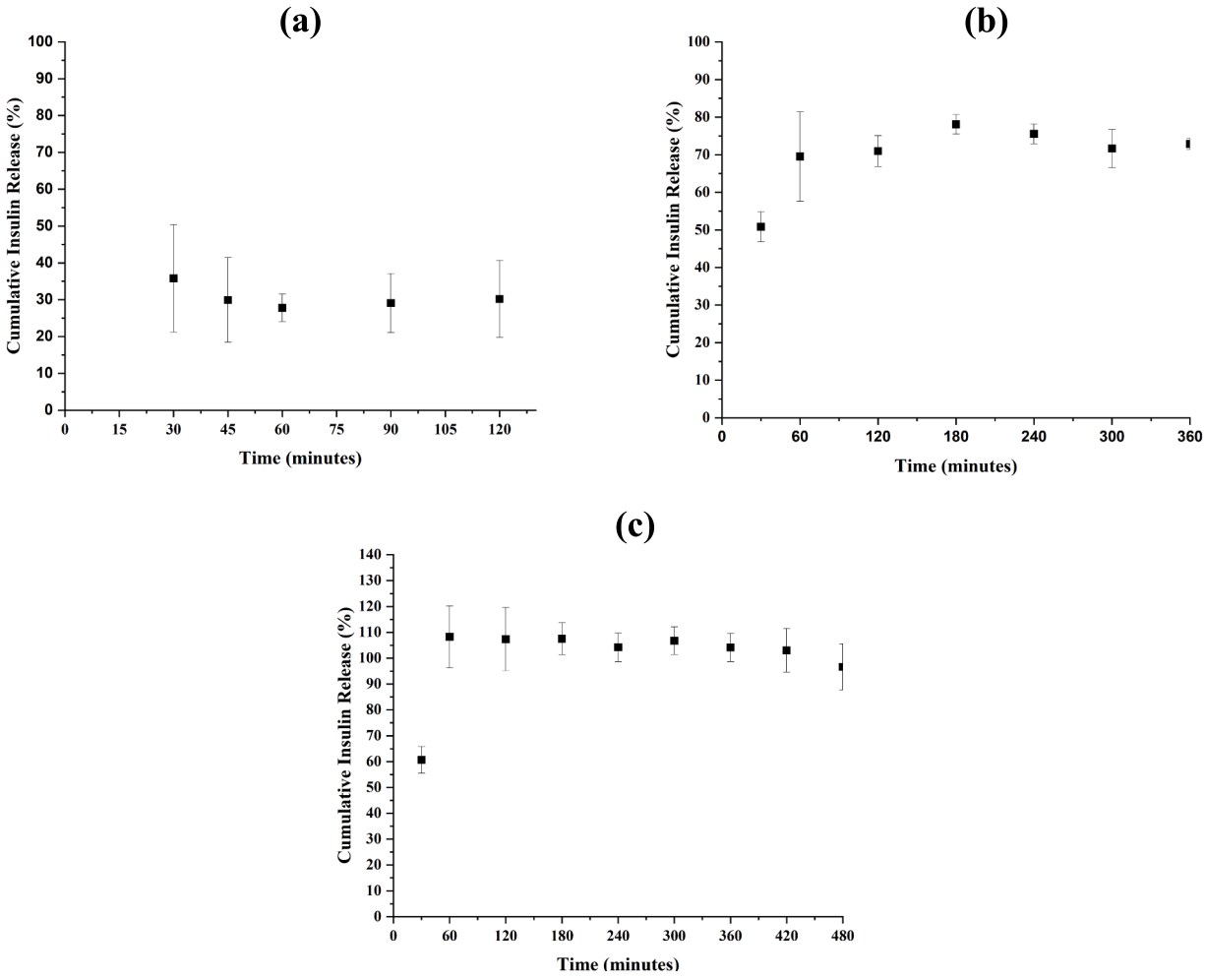

Fig. 8. Insulin release profiles from core-shell aerogel particles in (a) SGF, (b) SIF and (c) SCF media.

that the peak time for *Humulin R*® is typically between 2 and 3 h (Mayfield and Russell White, 2004).

The insulin release in the SCF medium takes place much faster than in SIF and reached 100 % within the first 120 min and slightly exceeded 100 % over time. The slight overshoot over 100 % could indicate measurement variability or a certain insulin degradation in slightly alkaline pH, while HPLC measurements lasted prolonged hours (Fagan et al., 2024). HPLC analysis confirmed the absence of chemical degradation of insulin in the aerogel formulation. In the next step of the study, after the optimization of the core–shell aerogel production process, the conformational stability of insulin will be checked using Circular Dichroism (CD) analysis to address this important aspect. Release results in SCF medium are consistent with previous studies with alginate-based carriers (Feyisa et al., 2023; Uyen et al., 2020; Wu et al., 2020). The efficient release in SCF medium highlights the potential of these aerogels for targeted colonic delivery. The drug delivery directly to the colon is promising for treating localized intestinal conditions and achieving systemic effects. Colon delivery might not be as efficient as absorbing drugs in the small intestine, but it offers some unique advantages, including a longer time for absorption, less enzyme activity that could break down drugs, and a better response to substances that enhance drug permeability (Illanes-Bordomás et al., 2023). These factors make the colon a potentially attractive route for improving the delivery of protein-based drugs like insulin. Given that colon-targeted insulin delivery is a relatively new area of research, this study represents a pioneering effort to examine how insulin (and other protein-based drugs/peptides) would be released in a simulated colonic environment.

Overall, the core–shell aerogels showed promising results for oral insulin delivery, with the ability to protect insulin in the stomach and release it effectively in the intestines and colon. Also, this is the first study to underscore the potential of aerogels as carriers for oral administration of insulin with targeted release in the colon.

4. Conclusions

Alginate-based core–shell aerogels show strong potential as effective carriers for oral insulin delivery, offering a non-invasive alternative to insulin subcutaneous injections. Results highlight the superior performance of the CS-B aerogel, attributed to its high specific surface area, optimal pore structure, and protective core–shell morphology. The release profiles of the drug-loaded core–shell aerogels in simulated gastric, intestinal and colonic fluids emphasized the controlled release capabilities of these aerogels. The minimum insulin release in SGF medium indicated robust stability and protection against the harsh acidic environment of the stomach. In SIF medium, an initial rapid release phase was observed followed by sustained release. This pattern aligns well with the pharmacokinetic requirements of regular/short-acting insulins like *Humulin R*®, effectively maintaining therapeutic insulin levels. The complete and rapid release in SCF medium suggests the potential for targeted colonic delivery, opening avenues for specific therapeutic applications for both regular/short-acting and rapid-acting insulin. The fine-tuning of alginate by the blending with chitosan used in this work has the potential to further enhance the performance of core–shell aerogels. Further research should focus on assessing their

scalability and increasing drug encapsulation efficiency to advance core–shell aerogel formulations towards clinical translation. The scope of this investigation can be expanded to include the encapsulation and release of other therapeutic agents (e.g., monoclonal antibodies for colorectal cancer) to determine the versatility of core–shell aerogels for diverse drug delivery applications.

CRediT authorship contribution statement

Gozde Ozesme Taylan: Writing – original draft, Visualization, Methodology, Investigation, Formal analysis, Conceptualization. **Carlos Illanes-Bordomás:** Writing – original draft, Methodology, Investigation, Conceptualization. **Ozge Guven:** Visualization, Investigation. **Ece Erkan:** Visualization, Investigation. **Sevil Çıkrıkcı Erünsal:** Writing – review & editing, Supervision. **Mecit Halil Oztop:** Writing – review & editing, Supervision, Project administration, Funding acquisition. **Carlos A. García-González:** Writing – review & editing, Supervision, Project administration, Methodology, Funding acquisition, Conceptualization.

Declaration of competing interest

The authors declare that they have no known competing financial interests or personal relationships that could have appeared to influence the work reported in this paper.

Acknowledgements

This work was funded by MICIU/AEI/10.13039/501100011033 [grant PID2020-120010RB-I00] and ERDF/EU, and carried out in the framework of the ECO-AERoGELS COST Innovators' Grant (ref. IG18125), the European Commission and TÜBİTAK Science Fellowship and Grant Programs Directorate (BİDEB) 2211-C National Scholarship Program in the Priority Fields in Science. C. I.-B. acknowledges MCINN and FSE+ for an FPI fellowship (PRE2021-097177/AEI/10.13039/501100011033).

Data availability

Data will be made available on request.

References

Abdul Khalil, H.P.S., Bashir Yahya, E., Jummaat, F., Adnan, A.S., Olaiya, N.G., Rizal, S., Abdullah, C.K., Pasquini, D., Thomas, S., 2023. Biopolymers based aerogels: a review on revolutionary solutions for smart therapeutics delivery. Prog. Mater. Sci. https://doi.org/10.1016/j.pmatsci.2022.101014.

Ajdary, R., Tardy, B.L., Mattos, B.D., Bai, L., Rojas, O.J., 2021. Plant nanomaterials and inspiration from nature: water interactions and hierarchically structured hydrogels. Adv. Mater. https://doi.org/10.1002/adma.202001085.

Alam, H., Ozesme Taylan, G., Yamali, C., Oztop, M.H., 2024. Synergistic quantification of mixed insulin preparations using time domain NMR techniques. J. Pharm. Biomed. Anal. 247. https://doi.org/10.1016/j.jpba.2024.116260.

Amin, M.K., Boateng, J.S., 2022. Enhancing stability and mucoadhesive properties of chitosan nanoparticles by surface modification with sodium alginate and polyethylene glycol for potential oral mucosa vaccine delivery. Mar. Drugs 20. https://doi.org/10.3390/md20030156.

Arbit, E., Kidron, M., 2017. Oral insulin delivery in a physiologic context: review. J. Diabetes Sci. Technol. 11, 825–832. https://doi.org/10.1177/1932296817691303.

Awoke, Y., Chebude, Y., Díaz, I., 2020. Controlling particle morphology and pore size in the synthesis of ordered mesoporous materials. Molecules 25. https://doi.org/10.3390/molecules25214909.

Balmforth, N.J., Craster, R.V., 2001. Geophysical Aspects of Non-Newtonian Fluid Mechanics, pp. 34–51. https://doi.org/10.1007/3-540-45670-8_2.

Bashir, S., Fitaihi, R., Abdelhakim, H.E., 2023. Advances in formulation and manufacturing strategies for the delivery of therapeutic proteins and peptides in orally disintegrating dosage forms, 106374 Eur. J. Pharm. Sci. 182. https://doi.org/10.1016/j.ejps.2023.106374.

Bensouiki, S., Belaib, F., Sindt, M., Magri, P., Rup-Jacques, S., Bensouici, C., Meniai, A. H., 2020. Evaluation of anti-inflammatory activity and in vitro drug release of ibuprofen-loaded nanoparticles based on sodium alginate and chitosan. Arab. J. Sci. Eng. 45, 7599–7609. https://doi.org/10.1007/s13369-020-04720-2.

Cao, J., Cheng, J., Xi, S., Qi, X., Shen, S., Ge, Y., 2019. Alginate/chitosan microcapsules for in-situ delivery of the protein, interleukin-1 receptor antagonist (IL-1Ra), for the treatment of dextran sulfate sodium (DSS)-induced colitis in a mouse model. Eur. J. Pharm. Biopharm. 137, 112–121. https://doi.org/10.1016/j.ejpb.2019.02.011.

Carracedo-Pérez, M., Ardao, I., López-Iglesias, C., Magariños, B., García-González, C.A., 2024. Direct and green production of sterile aerogels using supercritical fluid technology for biomedical applications. J. CO2 Util. 86. https://doi.org/10.1016/j.jcou.2024.102891.

Ching, A.L., Liew, C.V., Heng, P.W.S., Chan, L.W., 2008. Impact of cross-linker on alginate matrix integrity and drug release. Int. J. Pharm. 355, 259–268. https://doi.org/10.1016/j.ijpharm.2007.12.038.

Cikrikci, S., Mert, B., Oztop, M.H., 2018. Development of pH sensitive alginate/gum tragacanth based hydrogels for oral insulin delivery. J. Agric. Food Chem. 66, 11784–11796. https://doi.org/10.1021/acs.jafc.8b02525.

De Cicco, F., Russo, P., Reverchon, E., García-González, C.A., Aquino, R.P., Del Gaudio, P., 2016. Prilling and supercritical drying: a successful duo to produce core-shell polysaccharide aerogel beads for wound healing. Carbohydr. Polym. 147, 482–489. https://doi.org/10.1016/j.carbpol.2016.04.031.

El-Sherbiny, I.M., 2010. Enhanced pH-responsive carrier system based on alginate and chemically modified carboxymethyl chitosan for oral delivery of protein drugs: preparation and in-vitro assessment. Carbohydr. Polym. 80, 1125–1136. https://doi.org/10.1016/j.carbpol.2010.01.034.

Fagan, A., Bateman, L.M., O'Shea, J.P., Crean, A.M., 2024. Elucidating the degradation pathways of human insulin in the solid state. J. Anal. Test. https://doi.org/10.1007/s41664-024-00302-5.

Feyisa, Z., Gupta, N.K., Edossa, G.D., Sundaramurthy, A., Kapoor, A., Inki, L.G., 2023. Fabrication of pH-sensitive double cross-linked sodium alginate/chitosan hydrogels for controlled release of amoxicillin. Polym. Eng. Sci. 63, 2546–2564. https://doi.org/10.1002/pen.26395.

U.S. Food and Drug Administration, 2011. Humulin® R Regular Insulin Human Injection. Indianapolis.

García-González, C.A., Alnaief, M., Smirnova, I., 2011. Polysaccharide-based aerogels—promising biodegradable carriers for drug delivery systems. Carbohydr. Polym. 86, 1425–1438. https://doi.org/10.1016/J.CARBPOL.2011.06.066.

García-González, C.A., Jin, M., Gerth, J., Alvarez-Lorenzo, C., Smirnova, I., 2015. Polysaccharide-based aerogel microspheres for oral drug delivery. Carbohydr. Polym. 117, 797–806. https://doi.org/10.1016/j.carbpol.2014.10.045.

García-González, C.A., Sosnik, A., Kalmár, J., De Marco, I., Erkey, C., Concheiro, A., Alvarez-Lorenzo, C., 2021. Aerogels in drug delivery: From design to application. J. Control. Release 332, 40–63. https://doi.org/10.1016/j.jconrel.2021.02.012.

Illanes-Bordomás, C., Landin, M., García-González, C.A., 2023. Aerogels as carriers for oral administration of drugs: an approach towards colonic delivery. Pharmaceutics 15. https://doi.org/10.3390/pharmaceutics15112639.

Imanishi, S., Sawano, Y., Kurayama, F., Shibata, Y., Matsuyama, T., Ida, J., 2024. High-performance aminosilane-infused alginate capsules for sustained drug release. J. Appl. Polym. Sci. https://doi.org/10.1002/app.56034.

Iyer, G., Dyawanapelly, S., Jain, R., Dandekar, P., 2022. An overview of oral insulin delivery strategies (OIDS). Int. J. Biol. Macromol. https://doi.org/10.1016/j.ijbiomac.2022.03.144.

Jamshidnejad-Tosaramandani, T., Kashanian, S., Karimi, I., Schiöth, H.B., 2023. Synthesis of an insulin-loaded mucoadhesive nanoparticle designed for intranasal administration: focus on new diffusion media. Front. Pharmacol. 14. https://doi.org/10.3389/fphar.2023.1227423.

Khodaei, M.J., Candelino, N., Mehrvarz, A., Jalili, N., 2020. Physiological closed-loop control (PCLC) systems: review of a modern frontier in automation. IEEE Access 8, 23965–24005. https://doi.org/10.1109/ACCESS.2020.2968440.

Kulkarni, R.V., Boppana, R., Krishna Mohan, G., Mutalik, S., Kalyane, N.V., 2012. PH-responsive interpenetrating network hydrogel beads of poly(acrylamide)-g-carrageenan and sodium alginate for intestinal targeted drug delivery: Synthesis, in vitro and in vivo evaluation. J. Colloid Interface Sci. 367, 509–517. https://doi.org/10.1016/j.jcis.2011.10.025.

Levato, R., Jungst, T., Scheuring, R.G., Blunk, T., Groll, J., Malda, J., 2020. From shape to function: the next step in bioprinting. Adv. Mater. 32, 1906423. https://doi.org/10.1002/adma.201906423.

Li, Y., Wang, C., Luan, Y., Liu, W., Chen, T., Liu, P., Liu, Z., 2022. Preparation of pH-responsive cellulose nanofibril/sodium alginate based hydrogels for drug release. J. Appl. Polym. Sci. 139, 51647. https://doi.org/10.1002/app.51647.

Limenh, L.W., 2024. A review on oral novel delivery systems of insulin through the novel delivery system formulations: a review. SAGE Open Med 12, 1–11. https://doi.org/10.1177/20503121231225319.

Mayfield, J.A., Russell White, W.D., 2004. Insulin Therapy for Type 2 Diabetes: Rescue, Augmentation, and Replacement of Beta-Cell Function.Am. Fam. Physician 70, 489–500.

Namli, S., Guven, O., Simsek, F.N., Gradišek, A., Sumnu, G., Yener, M.E., Oztop, M., 2023. Effects of deacetylation degree of chitosan on the structure of aerogels. Int. J. Biol. Macromol. 250, 126123. https://doi.org/10.1016/j.ijbiomac.2023.126123.

Nandiyanto, A.B.D., Ragadhita, R., Fiandini, M., 2023. Interpretation of Fourier transform infrared spectra (FTIR): a practical approach in the polymer/plastic thermal decomposition. Indonesian J. Sci. Technol. 8, 113–126. https://doi.org/10.17509/ijost.v8i1.53297.

Nenni, M., 2021. Determination of Insulin in saline by RP-HPLC combined with UV. Hacettepe University Journal of the Faculty of Pharmacy 41, 74–81. https://doi.org/10.52794/hujpharm.901476.

Pereira, R., Tojeira, A., Vaz, D.C., Mendes, A., Bártolo, P., 2011. Preparation and characterization of films based on alginate and aloe vera. Int. J. Polym. Anal. Charact. 16, 449–464. https://doi.org/10.1080/1023666X.2011.599923.

Poudwal, S., Misra, A., Shende, P., 2021. Role of lipid nanocarriers for enhancing oral absorption and bioavailability of insulin and GLP-1 receptor agonists. J. Drug Target. https://doi.org/10.1080/1061186X.2021.1894434.

Rashedy, S.H., Abd El Hafez, M.S.M., Dar, M.A., Cotas, J., Pereira, L., 2021. Evaluation and characterization of alginate extracted from brown seaweed collected in the red sea. Appl. Sci. 11, 6290. https://doi.org/10.3390/app11146290.

Sarmento, B., Ferreira, D., Veiga, F., Ribeiro, A., 2006. Characterization of insulin-loaded alginate nanoparticles produced by ionotropic pre-gelation through DSC and FTIR studies. Carbohydr. Polym. 66, 1–7. https://doi.org/10.1016/j.carbpol.2006.02.008.

Shu, X.Z., Zhu, K.J., 2002. Controlled drug release properties of ionically cross-linked chitosan beads: the influence of anion structure. Int. J. Pharm. 233, 217–225. https://doi.org/10.1016/S0378-5173(01)00943-7.

Siram, K., Habibur Rahman, S.M., Balakumar, K., Duganath, N., Chandrasekar, R., Hariprasad, R., 2019. Pharmaceutical nanotechnology: Brief perspective on lipid drug delivery and its current scenario. In: Biomedical Applications of Nanoparticles. Elsevier, pp. 91–115. DOI: 10.1016/B978-0-12-816506-5.00005-X.

Thomas, D., Mathew, N., Nath, M.S., 2021. Starch modified alginate nanoparticles for drug delivery application. Int. J. Biol. Macromol. 173, 277–284. https://doi.org/10.1016/j.ijbiomac.2020.12.227.

Tkalec, G., Knez, Ž., Novak, Z., 2016. PH sensitive mesoporous materials for immediate or controlled release of NSAID. Micropor. Mesopor. Mater. 224, 190–200. https://doi.org/10.1016/j.micromeso.2015.11.048.

Uyen, N.T.T., Hamid, Z.A.A., Tram, N.X.T., Ahmad, N., 2020. Fabrication of alginate microspheres for drug delivery: a review. Int. J. Biol. Macromol. 153, 1035-1046. https://doi.org/10.1016/j.ijbiomac.2019.10.233.

Valentin, R., Bonelli, B., Garrone, E., Di Renzo, F., Quidnard, F., 2007. Accessibility of the functional group of chitosan aerogel probed by FT-IR-monitored deuteration. Biomacromolecules 8, 3646–3650. https://doi.org/10.1021/bm070391a.

Ways, T.M.M., Lau, W.M., Khutoryanskiy, V.V., 2018. Chitosan and its derivatives for application in mucoadhesive drug delivery systems. Polymers 10, 267. https://doi.org/10.3390/polym10030267.

Wu, T., Yu, S., Lin, D., Wu, Z., Xu, J., Zhang, J., Ding, Z., Miao, Y., Liu, T., Chen, T., Cai, X., 2020. Preparation, characterization, and release behavior of doxorubicin hydrochloride from dual cross-linked chitosan/alginate hydrogel beads. ACS Appl. Bio Mater. 3, 3057–3065. https://doi.org/10.1021/acsabm.9b01119.

Zatorska, M., Łazarski, G., Maziarz, U., Wilkosz, N., Honda, T., Yusa, S. ichi, Bednar, J., Jamróz, D., Kepczynski, M., 2020. Drug-loading capacity of polylactide-based micro- and nanoparticles – Experimental and molecular modeling study. Int J Pharm 591. https://doi.org/10.1016/j.ijpharm.2020.120031.

Zhang, Y., Xiong, G.M., Ali, Y., Boehm, B.O., Huang, Y.Y., Venkatraman, S., 2021. Layer-by-layer coated nanoliposomes for oral delivery of insulin. Nanoscale 13, 776–789. https://doi.org/10.1039/d0nr06104b.